Carbohydrate Polymers 92 (2013) 775–783

Contents lists available at SciVerse ScienceDirect

Carbohydrate Polymers

journal homepage: www.elsevier.com/locate/carbpol

Preparation of dry ultra-porous cellulosic fibres: Characterization and possible initial uses

Anna Svensson[a,*], Per Tomas Larsson[a,b], German Salazar-Alvarez[a,c], Lars Wågberg[a,d,**]

[a] Wallenberg Wood Science Center, KTH Royal Institute of Technology, Stockholm, Sweden
[b] Innventia AB, Stockholm, Sweden
[c] Department of Material & Environmental Chemistry, Arrhenius Lab, Stockholm University, Stockholm, Sweden
[d] Fibre and Polymer Technology, KTH Royal Institute of Technology, Stockholm, Sweden

ARTICLE INFO

Article history:
Received 6 July 2012
Received in revised form 29 August 2012
Accepted 28 September 2012
Available online 8 October 2012

Keywords:
Cellulose fibre
Composite
In situ polymerization
Liquid exchange
Open structure
Surface area

ABSTRACT

Dry ultra-porous cellulose fibres were obtained using a liquid exchange procedure in which water was replaced in the following order: water, methanol, acetone, and finally pentane; thereafter, the fibres were dried with Ar(g). The dry samples (of TEMPO-oxidized dissolving pulp) had a specific surface area of 130 $m^2 g^{-1}$ as measured using BET nitrogen gas adsorption. The open structure in the dry state was also revealed using field emission scanning electron microscopy.

This dry open structure was used as a scaffold for in situ polymerization. Both poly(methyl methacrylate) and poly(butylacrylate) were successfully used as matrix polymers for the composite material (fibre/polymer), comprising approximately 20 wt% fibres. Atomic force microscopy phase imaging indicated a nanoscale mixing of the matrix polymer and the cellulose fibril aggregates and this was also supported by mechanical testing of the prepared composite where the open fibre structure produced superior composites. The fibre/polymer composite had a significantly reduced water absorption capacity also indicating an efficient filling of the fibre structure with the matrix polymer.

1. Introduction

Over the last ten years, interest has mounted in the development of materials from renewable resources, spurred by awareness of future shortages of raw materials. In this context, cellulose fibrils and nanocrystals have been the subject of considerable interest, both because of the development of new, efficient preparation processes (Eichhorn et al., 2010; Klemm et al., 2011) and because cellulose is the most common natural polymer on earth. Given the achievements of nanotechnology and the small dimensions of this material, it is clear that these building blocks can be used both as reinforcing element in composite materials and in high-value-added interactive products (Hsu, Weder, & Rowan, 2011; Mendez et al., 2011; Olsson et al., 2010).

Despite all the advantages of using nano sized cellulose, the preparation of these materials demands different types of processing and, although these methods have been developed, they are still costly and result in dispersions with fairly low concentrations of NFC and CNC. Further on, when utilizing nano sized cellulose as reinforcing element in composites, it is difficult to obtain good dispersion of it in a hydrophobic polymeric matrix and different approaches to handle this problem have been explored (Belgacem & Gandini, 2008).

One way to prepare composite material with nano cellulose as reinforcing element was presented by Capadona et al. (2007). They formed a template, or scaffold, of cellulose nano whiskers in water and after a liquid exchange, a gel of nano whiskers was formed with the whiskers arranged in a percolating 3D structure. The template was thereafter immersed in to a polymer solution, allowing the template to be filled with the matrix polymer before drying of the composite.

Since a delignified fibre wall has a remarkably high specific surface area in water swollen state it should be possible to utilize this great property by using the open fibre wall structure as a scaffold, in a similar way as in the work by Capadona et al. (2007). Such a fibre wall comprises of approximately 100 lamellae (Stone & Scallan, 1965) of cellulose fibrils, 20 nm × 20 nm in cross-section and more than 1 μm in length (Hult, Larsson, & Iversen, 2001). If the open fibre wall is used as a scaffold, and thereafter filled with a polymeric matrix, a composite could be formed with nano sized cellulose as reinforcing element without the disintegration step performed. Despite the obvious advantages of this procedure it has not, to the knowledge of the authors, been evaluated earlier.

* Corresponding author at: Wallenberg Wood Science Center, KTH-Teknikringen 56, SE-100 44 Stockholm, Sweden. Tel.: +46 8 790 8036; fax: +46 8 790 8066.
** Corresponding author at: Fibre and Polymer Technology, KTH-Teknikringen 56-58, SE-100 44 Stockholm, Sweden. Tel.: +46 8 790 8294; fax: +46 8 790 6166.
E-mail addresses: annas2@kth.se (A. Svensson), wagberg@kth.se (L. Wågberg).

0144-8617/$ – see front matter © 2012 Elsevier Ltd. All rights reserved.
http://dx.doi.org/10.1016/j.carbpol.2012.09.090

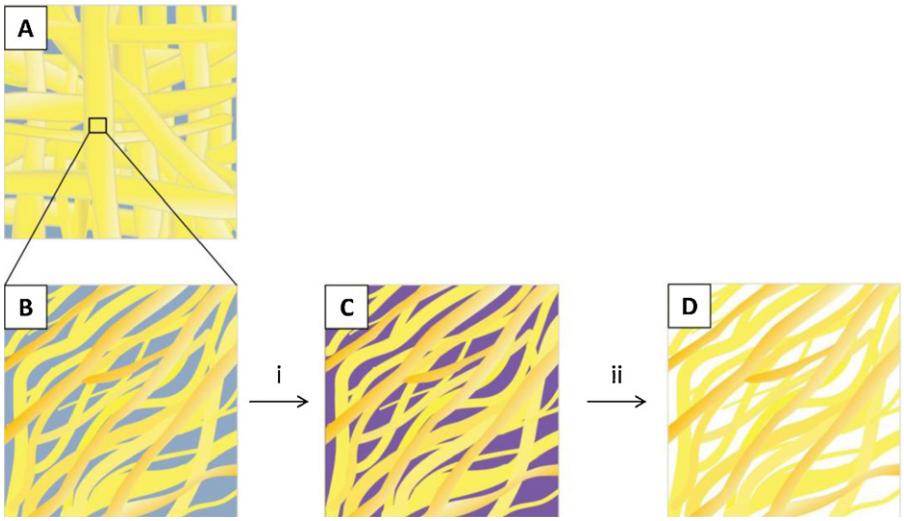

Fig. 1. Schematic presentation of the preservation of the open fibrous structure. Initially a fibre network is formed as a regular hand sheet (A). (B) is an enlargement of (A) and illustrates how the cellulose fibril aggregates are separated from each other in the water-swollen state of the delignified fibre wall. By replacing the water, light blue coloured in (B), with a less polar liquid, dark blue coloured in (C), and thereafter carefully drying the sample while avoiding contact with humidity in air, the open structure can be preserved in the dry state. The white colour of the pores in (D) illustrates the dry state.

A conventionally dried cellulose fibre has, as a comparison, a specific surface area of 1 $m^2 g^{-1}$ whereas the open cellulose fibre has a specific surface area around 100 $m^2 g^{-1}$.

In order to functionalize the fibre wall in such a way, chemicals, monomers, polymers, inorganic starting materials, etc., need to enter the pores in the fibre wall, i.e., have dimension smaller than the distance between the fibrils in the water-swollen fibre wall, which is approximately 15–45 nm (Andreasson, Forsström, & Wågberg, 2005; Duchesne & Daniel, 1999). If the fibre is kept in water, the choice of substance to fill the fibre wall with will be limited by substances that can be dissolved in water. On the other hand, if the open fibre structure is preserved in dry state, the dry fibre can be functionalized with anything of choice, regardless polarity, as long as the substances are small enough to enter the pores. This procedure would then allow for preparation of materials built up of nano sized cellulose that are mixed with a matrix regardless of its polarity, i.e., both the disintegration step and the mixing problem mentioned above would be circumvented.

Preserving and using the open, wet fibre structure in the dry state would create completely new possibilities for preparing nanocomposite materials, structured all the way from the nano-level up to macroscopic properties of fibrous materials. If the open structure of the fibres can be preserved within a macroscopic paper, it should be possible to do similar particle deposition on the fibrils in the intact fibre wall while retaining the great advantages of forming large-scale fibrous networks using regular sheet-making methods.

The challenge is naturally to preserve the open structure in the formed sheet after preparation but before final drying, since it is well known that the air-dried fibre wall has a very compact structure with basically no free pores (Stone & Scallan, 1965). Liquid exchange of fibres and pulp has been done earlier, often in order to see how different process steps affect the closure of pores in the fibre wall during drying and as well in order to achieve more knowledge of the fibre wall structure (Herrington & Midmore, 1984; Kohnke, Lund, Brelid, & Westman, 2010). To our knowledge, this is the first time the liquid exchange procedure has been performed on fibre sheet, in order to obtain a scaffold of the open fibre structure and to utilize it in functionalized materials later on. A large effort of the present work has therefore been to establish a robust drying method, including liquid exchange with liquids of successively lower polarity, while retaining the open structure of the fibre wall in a paper sheet; see Fig. 1 for a schematic of the method. The structure of the fibre wall in its water-swollen state (see Fig. 1B) was characterized using solid-state nuclear magnetic resonance (NMR) (Chunilall, Bush, Larsson, Iversen, & Kindness, 2010) and the dry structure after liquid exchange and drying (see Fig. 1D) was characterized using BET nitrogen gas adsorption (Brunauer, Emmett, & Teller, 1938) and field emission scanning electron microscopy (FE-SEM).

In order to explore the possibility to use the dry open fibre structure as a scaffold, a composite material can be prepared. Considering the size of the pores in the fibre wall, an in situ polymerization is a good alternative to polymerize the composite matrix since monomer will have no difficulty to enter through the preserved pores. If the dry open fibres are oriented in a fibre network structure and the whole network structure is used as scaffold, impregnated with monomer before initiating the polymerization, both fibrils and fibres would be ideally mixed with the matrix polymer (see Fig. 2). The composite would not be reinforced by fibres, as conventionally fibre-reinforced composites, but instead by the nano sized fibrils in the fibre wall and this achieved without the need to first disintegrate the fibre wall. The composite would therefore be classified as a nano composite rather than a micro composite. Furthermore, stress concentrations at the fibre ends would not be a problem, since the polymer would be interpenetrated into the fibrillar structure of the entire fibre wall.

The latter approach was evaluated in the present work and two different monomeric systems were tested, methylmethacrylate (MMA) and butyl acrylate (BA), both in situ polymerized in the preserved open fibrillar structure of fibre sheets, and composite materials were formed; fibre/PMMA and fibre/PBA. The structure of these composites was analysed using FE-SEM and atomic force microscopy (AFM). The mechanical properties and also the water absorption capacity of the composite material were determined, the latter in order to estimate the pore volume of the composite when exposed to liquid water.

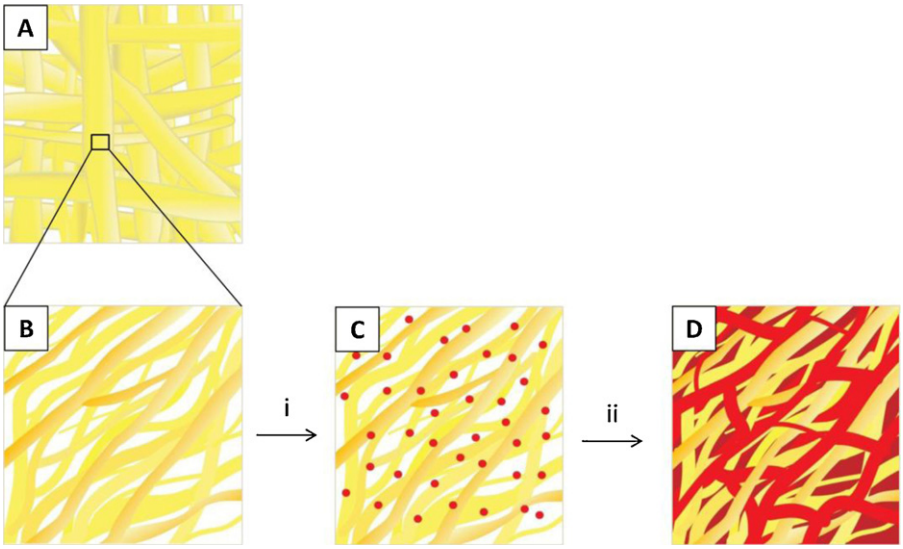

Fig. 2. Schematic presentation of how the dry fibre sheet (A) consisting of fibres with an open fibrillar structure (B) was used as scaffold for in situ polymerization. The open structure of fibre wall in dry state (B) makes it possible for the monomers to penetrate into the porous structure of the fibre wall (C). After this, an in situ polymerization was initiated, creating an interpenetrating polymer network (D) that mixes polymer matrix and cellulose aggregates on the nanometer scale.

2. Experimental

2.1. Materials

Two fibre sources were used for the sheet preparation: a never-dried sulphate kraft pulp from SCA Östrand AB, Sundsvall, Sweden, and a never-dried dissolving pulp from Domsjö Fabriker AB, Örnsköldsvik, Sweden. The sulphate pulp was converted into its sodium form (Wågberg & Björklund, 1993) before sheet preparation. The dissolving pulp was first oxidized with TEMPO at neutral pH (Saito et al., 2009), to a charge density of approximately 600 $\mu eq\, g^{-1}$ and thereafter converted into its sodium form to establish a ground state for the dissociation of the carboxyl groups (Wågberg & Björklund, 1993).

For the TEMPO oxidation, the following chemicals were used: $NaClO_2$ (puriss p.a.), NaClO (10% solution), 2,2,6,6-tetramethyl-1-piperidinyloxy (TEMPO; free radical). All chemicals were purchased from Sigma–Aldrich Sweden AB, Stockholm, Sweden, and used as supplied by the manufacturer.

For the liquid exchange, the following liquids were used as supplied by the manufacturer: Methanol (general purpose grade, methanol (aq) >70%), acetone (analytical reagent grade) and pentane (>99%). All liquids were used as received. Methanol and acetone were purchased from Fisher Scientific, Göteborg, Sweden and pentane was purchased from VWR International AB, Stockholm, Sweden.

The following chemicals were used for polymerization: methyl methacrylate (MMA, >97%) and butyl acrylate (BA, 99+%) were passed through a basic alumina column before use. α,α′-Azoisobutyronitril (AIBN, for synthesis) and tri(propylene glycol) diacrylate (TPGDA, technical grade) were both used as supplied by the manufacturer. MMA, BA and TPGDA were purchased from Sigma–Aldrich Sweden AB, Stockholm, Sweden and AIBN was purchased from Merck, Darmstadt, Germany.

2.2. TEMPO-mediated oxidation of never-dried dissolving pulp

For the TEMPO oxidation, the basic procedure described by Saito et al. (2009) was used. The never-dried dissolving pulp was first purified with 0.3% $NaClO_2$ in acetate buffer (40 mL of acetate buffer per gram of dry pulp) at pH 4.6 and 60 °C for 1 h, after which the pulp was washed with deionized water by filtration. The pulp was thereafter dispersed in phosphate buffer (90 mL of phosphate buffer per gram of dry fibre) at pH 6.8 and 60 °C. $NaClO_2$ (10 mmol, 80%), TEMPO (0.1 mmol) and NaClO (1.0 mmol), the amounts of chemicals calculated per g of fibre, were added to the flask and the dispersion was stirred for 2 h 20 min. The pulp was thereafter washed with deionized water by filtration. The charge density of the pulp was determined to be 600 $\mu eq\, g^{-1}$ using conductometric measurement (Katz, Beatson, & Scallan, 1984). The pulp was then washed into its sodium form before sheet preparation.

2.3. Formation of a dry ultra-porous fibre network

The never-dried pulps were dispersed in deionized water and sheets with a grammage of approximately 110 $g\, m^{-2}$ were prepared using a Rapid Köthen sheet-forming device (PTI, Vorchdorf, Austria). The sheets were dried for only 2 min 30 s under a reduced pressure of 95 kPa to get rid of excess water for the following liquid exchange procedure.

The sheets, still wet with water from the sheet-making process, were cut into smaller samples 1 cm × 5 cm in size. The water in the samples was gradually replaced with successively less polar liquids in the following order: water, methanol, acetone, and finally pentane. The concentration of fibres in liquid was approximately 1% and each liquid was exchanged ten times over two days before the samples were subjected to a new liquid.

The sheets were dried from pentane in two ways: the kraft pulp samples were frozen in liquid nitrogen and then freeze dried (FD), while the dissolving pulp samples were dried in a stream of argon gas for one night.

The liquid exchange procedure was inspired by earlier work (Herrington & Midmore, 1984; Kohnke et al., 2010; Wang, Maloney, & Paulapuro, 2003). Both kinds of samples were stored in a well-sealed vessel to avoid contact with humid air.

As a reference, samples of the dissolving pulp were dried as conventional hand sheets, i.e., dried from water directly after sheet preparation.

2.4. Measurement of specific surface area in the water-swollen state using solid-state NMR

The TEMPO-oxidized dissolving pulp needed extra treatment before performing solid-state NMR measurement on the wet samples. The following treatment was applied in order to reduce the ionic strength of the sample liquid present during measurement. The fibre suspension was first adjusted to pH 2, according to the procedure mentioned earlier (Wågberg & Björklund, 1993), and thereafter the pH of the fibre suspension was adjusted to 3.5.

All samples were wetted with deionized water to 40–60% water content and packed uniformly in a zirconium oxide rotor. Recording spectra on wet samples gives a higher apparent resolution than does using dry samples (Newman, 1992). The cross-polarization magic angle spinning (CP/MAS) ^{13}C NMR spectra were recorded in a Bruker Avance III AQS 400 SB instrument operating at 9.4 T. All measurements were performed at 295 (±1) K. The MAS rate was 10 kHz. A 4 mm double-air-bearing probe was used. Acquisition was performed using a CP pulse sequence, with a 2.95 μs proton 90° pulse, an 800 μs ramped (100–50%) falling contact pulse, and a 2.5 s delay between repetitions. A SPINAL64 pulse sequence was used for ^{1}H decoupling. The Hartman–Hahn matching procedure is based on glycine. The chemical shift scale was calibrated to the TMS ($(CH_3)_4Si$) scale by assigning the data point of maximum intensity in the glycine carbonyl signal to a shift of 176.03 ppm; 4096 transients were recorded on each sample giving an acquisition time of approximately 3 h. The software for spectral fitting was made by Innventia AB and is based on a Levenberg–Marquardt algorithm (Larsson, Wickholm, & Iversen, 1997). All computations were based on integrated signal intensities as obtained from the spectral fitting (Wickholm, Larsson, & Iversen, 1998). The cellulose I specific surface area was calculated from the lateral fibril aggregate dimensions by assigning a density of 1500 kg m^{-3} to cellulose I (Chunilall et al., 2010).

2.5. Measurement of specific surface area in the dry state using gas adsorption and BET analysis

The surface area ($m^2\,g^{-1}$), according to Brunauer–Emmett–Teller (BET) analysis (Brunauer et al., 1938), was determined using N_2 physisorption with a Micromeritics ASAP 2020 analyser for samples treated according to the liquid exchange procedure (described in Section 2.3) and for the conventionally dried reference sample.

2.6. Field-emission scanning electron microscopy (FE-SEM)

The open fibrillar structure (Fig. 3) was covered with gold–palladium using an Agar HR sputter coater to a thickness of 8 nm and thereafter analysed using FE-SEM (Hitachi S-4800). The fibre/PMMA cross-section (Fig. 5A) was also analysed using the same microscopy technique.

Specimens of fibre/PMMA (Fig. 5B) and fibre/PBA (Fig. 5C) were coated with carbon (SCD 005, Balzers, Liechtenstein). The specimens were analysed in an Ultra 55 FE-SEM (Carl Zeiss, Oberkochen, Germany) at 3 kV.

2.7. Biocomposite preparation by in situ polymerization of matrix polymer in the open fibrillar structure

The dry fibre samples, treated according to the liquid exchange procedure, were immersed into a mixture of monomer (MMA or BA), cross-linker (TPGDA) and initiator (AIBN). The mixture consisted of 90 mol% of monomer, 10 mol% of cross-linker and 2.5 wt% of initiator, and the three compounds were mixed for 5 min in a vial before fibre sample immersion. After one day in the mixture, the samples were taken out and excess mixture was removed using filter paper. The samples were thereafter placed between two glass plates covered with Teflon film. The glass plates were held together by clamps, exerting mechanical pressure on the fibre samples during polymerization. The polymerization was initiated by heating the samples at 80 °C for 2 h in an oven. The composites are denoted fibre/PMMA and fibre/PBA or, more generally, simply fibre/polymer.

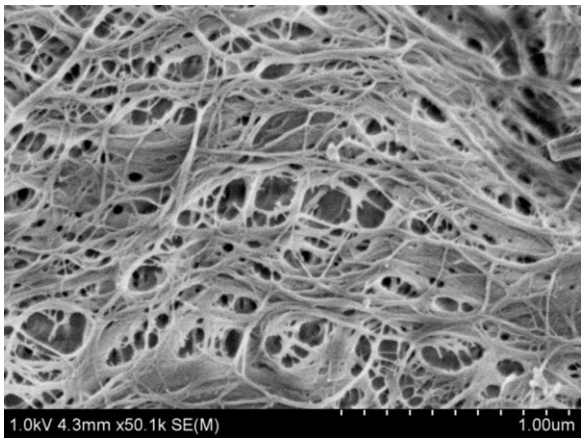

Fig. 3. SEM image of the open fibre wall structure of the TEMPO-oxidized dissolving pulp after liquid exchange and drying. The scale bar in the image indicates 1 μm.

As a reference, composites were prepared from sheets air dried from water and thereafter immersed into a mixture with the same proportions of constituents as mentioned earlier and polymerized in the same way as described above. The reference samples are denoted fibre/PMMA WD and fibre/PBA WD, or, more generally, fibre/polymer WD, WD indicating that the fibres were dried from water.

2.8. Atomic force microscopy (AFM)

Both composites (i.e., fibre/PMMA and fibre/PBA) were embedded in epoxy resin (Spurr's resin; TAAB Laboratories Equipment, Aldermaston, UK) and cured for 24 h at 60 °C. The samples were cut in a rotary microtome and thereafter analysed using a Nanoscope IIIa AFM (Bruker AXS, formerly Veeco Instruments, Santa Barbara, USA) equipped with a type E piezoelectric scanner. The images were acquired in tapping mode using an MSNL cantilever (Veeco Instruments, Plainview, NY) with a normal spring constant of 0.3 N m^{-1} and a tip radius of 2 nm.

2.9. Water absorption capacity

Samples of composites were cut into smaller pieces and soaked in water for three days. Excess water was removed with blotting paper before the samples were dried in oven over night at 105 °C. Wet and dry samples, i.e., before and after drying, were weighed to determine the water content of the treated sheets.

2.10. Mechanical properties

Mechanical properties of the composite material were investigated by means of tensile testing. The measurements were made using an Instron 5566 Universal Material Testing Machine (Instron, Grove City, PA) equipped with a 2 kN load cell. The cross head speed was 2 mm min^{-1} and the stress–strain curves were recorded. The samples, 20 mm long, 10 mm wide, and with a thickness of 260–580 μm were stored at 50% R.H. and 23 °C for at least one

Table 1
Comparison of specific surface area measured using NMR for water-swollen samples and using BET for dry samples, after liquid exchange and drying.

Pulp	Surface area [$m^2 g^{-1}$], water-swollen state NMR	Liquid exchange, drying	Surface area [$m^2 g^{-1}$], dry state BET
Kraft	100	Water, methanol, acetone, pentane, FD	128
Diss.	158	Water, methanol, acetone, pentane, Ar(g)	75
Diss.	158	Air dried from water	1.6
Diss.-TO	135	Water, methanol, acetone, pentane, Ar(g)	130

night before testing. Four or five samples of each composite were measured.

3. Results

3.1. Preservation of pore structure during drying

The specific surface area measurements made using NMR (water-swollen state) and BET (dry state) are presented in Table 1.

The NMR measurements, which convey information about the supramolecular structure in the water-swollen state, indicated that the dissolving pulp had a higher specific surface area (158 $m^2 g^{-1}$) than did the kraft pulp (100 $m^2 g^{-1}$). The TEMPO-oxidized dissolving pulp had a lower specific surface area (135 $m^2 g^{-1}$) than did the non-oxidized dissolving pulp (158 $m^2 g^{-1}$).

After liquid exchange and drying, both the kraft pulp and the TEMPO-oxidized dissolving pulps gave similar BET measurement values, i.e., 128 $m^2 g^{-1}$ and 130 $m^2 g^{-1}$, respectively. As expected, the sample of dissolving pulp dried from water had a small specific surface area of 1.6 $m^2 g^{-1}$.

Since the TEMPO-oxidized dissolving pulp had the greatest specific surface area in the dry state, this pulp was chosen for further experimental work. This pulp will be denoted as "fibre" in the context of composite materials later on.

The structure of the dry fibre wall of the liquid-exchanged TEMPO-oxidized dissolving pulp was also investigated using SEM. The image shows partly aggregated fibrils and pores of various sizes, as well as many open spaces larger than 20 nm, see Fig. 3.

3.2. Preparation of interpenetrating fibril and polymer network

Composite materials were obtained for both polymer matrixes, i.e., fibre/PMMA and fibre/PBA, using the dry porous fibres as scaffolds for in situ polymerization. The composites consisted of approximately 20 wt% fibres and were fairly transparent (see Fig. 4A for fibre/PBA and Fig. 4B for fibre/PMMA). Fig. 4C is the reference fibre/PMMA WD, i.e., fibres dried from water in air.

The composites were also analysed using SEM (see Fig. 5). Image A shows the cross-section of the fibre/PMMA composite, in which the cut is perpendicular to the *xy*-plane of the sheet and the transverse cross-sections of fibres can clearly be seen. The fibres are unevenly distributed in the PMMA matrix and the image reveals that the fibres are filled with the polymer. Images B and C, taken with higher magnification of the individual fibres (i.e., not a cross-section of the composite), show cellulose fibril aggregates covered by the polymer matrix.

AFM images of a cross-section of a fibre in fibre/PMMA are presented in Fig. 6. Image A is an AFM height image and shows a cross-section of a fibre in the polymer matrix. The corresponding surface roughness profile, presented below image A, indicates a flat area surrounded by rougher areas. The surface profile was acquired along a line extending from the lower-left corner towards the middle of the right side; the two crosses in image A correspond to the dotted vertical lines in the surface roughness profile. Two phase images were taken from the same sample. Image B was taken from the left part of the fibre wall and image C from the right part of the fibre wall. It is obvious that two different phases are represented in these phase images.

The water absorption capacity of the composites was also determined, to yield insight into the efficiency of the polymer/fibril interpenetration during the in situ polymerization. If the fibre wall is completely filled with polymer, water uptake should be very limited. The results of these water absorption capacity measurements are presented normalized with respect to both the sample weight and fibre weight of the composite. Results for both fibre/PMMA and fibre/PBA as well as for the reference samples are presented in Table 2.

Both fibre/PMMA and fibre/PBA have significantly reduced abilities to absorb water compared with the reference samples.

The stress–strain behaviour of the materials is presented in Fig. 7. The composites prepared by in situ polymerization of the dry open fibre structure, i.e., fibre/PMMA and fibre/PBA, are shown in black. The reference samples, i.e., fibre/PMMA WD and fibre/PBA WD, are shown in grey in each graph.

Note that the fibre content (in wt%) of samples containing fibres treated using the liquid exchange method differs from that of samples containing fibres dried from water in air, since similar wt% of fibres in the samples was very difficult to achieve without altering the structure of the open fibre wall.

Fibre/PMMA has both a higher modulus and tensile stress but a lower strain at break than the reference fibre/PMMA WD. Fibre/PBA has a higher tensile stress and an improved strain

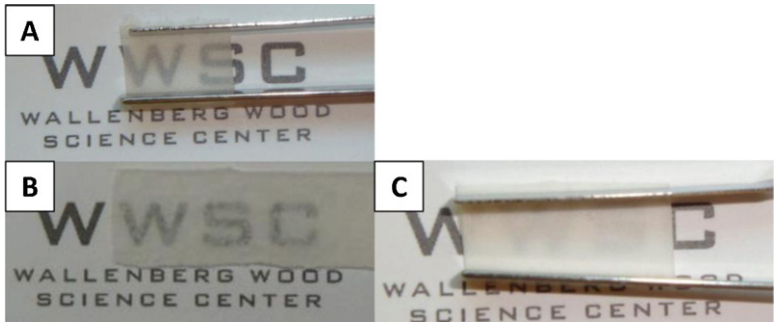

Fig. 4. Photographs of in situ polymerized fibre-reinforced composites. Image A represents fibre/PBA and image B fibre/PMMA composites. For both samples, the matrix polymer was in situ polymerized in the dry open fibrillar structure. The weight% of fibres was approximately 20 wt% for both samples. Image C is the reference containing fibres dried from water, i.e., fibre/PMMA WD; this sample contained approximately 60 wt% fibres.

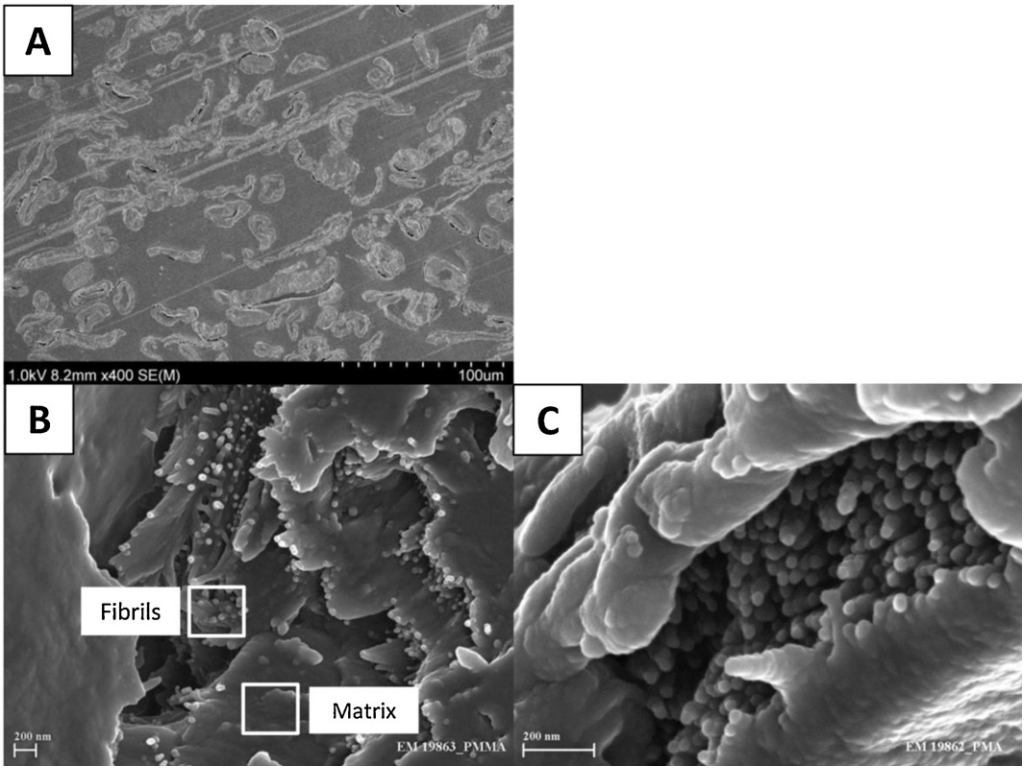

Fig. 5. SEM images of in situ polymerized fibre-reinforced composites: image A is a cross-section of fibre/PMMA (scale bar, 100 μm), image B shows a fibre in fibre/PMMA (scale bar, 200 nm), and C shows a fibre in fibre/PBA (scale bar, 200 nm). Fibrils and matrix are marked in image B.

at break, but a lower modulus than the reference fibre/PBA WD.

4. Discussion

4.1. Critical parameters for preserving the wet porous structure

Both pulps used in this work were never-dried pulps, since rewetting of hornified fibres cannot re-swell the fibres to the same degree as in never-dried pulps (Stone & Scallan, 1966). The two pulps have different cellulose contents; in general, dissolving pulp contains 95% cellulose, whereas kraft pulp contains approximately 85% cellulose, the rest mainly being hemicellulose.

The liquid exchange procedure aims to preserve the open structure the fibre wall has in its water-swollen state. Liquid exchange of fibres has indeed been performed before, mainly in order to follow structural changes of the fibre during drying or in order to preserve the water swollen structure in dry state for the sake of its characterization. For instance, Kohnke et al. (2010) adsorbed glucuronoxylan onto cellulose in order to prevent fibre hornification. Their reference samples, never-dried bleached softwood kraft pulp with no extra adsorbed glucuronoxylan, had a specific surface area of approximately 150 $m^2\ g^{-1}$ measured with BET. Another example of liquid exchange is the work done by Herrington and Midmore (1984). They compared the results of specific surface area measured by negative co-ion adsorption of water swollen samples and by BET of dry samples. As an example of their results, a never-dried bleached sulphate pulp had a specific surface area of 190 $m^2\ g^{-1}$. The earlier published work summarised here shows that our results of specific surface area measured of dry fibres are in agreement with earlier results. Although, the liquid exchange and drying procedure performed in this work, aims for a new purpose since the dry open fibre structure is intended to serve as a scaffold for functionalized materials. To our knowledge, this is the first time this concept in combination with the preservation of a fibre network structure has been explored. Especially where the fibres have been pre-formed into a sheet to allow for the preparation of a 2D oriented composite.

If the supramolecular structure is changed in the water-swollen state, it is strongly believed that the structure preserved in the dry state will be affected by that change as well. The TEMPO-mediated oxidation of the dissolving pulp was performed to introduce charges on the glucan chain and thereby increase the fibre swelling in water (Lindström & Carlsson, 1982).

By comparing the specific surface area values as measured using NMR and BET, it is possible to evaluate the liquid exchange procedure. During the procedure, the water is replaced with successively less polar liquids to prevent fibre wall collapse and to allow for liquid removal without creating pore closure. In this procedure, it is vital that contact with humid air must be prevented during drying. Ideally, the entire available surface in the water-swollen state would be preserved in the dry state, but it is difficult to completely prevent pore contraction during sample handling before analysis.

The theoretical model used for calculating the specific surface area from NMR spectra recorded for water-swollen fibres assumes that the material consists of pure cellulose (Chunilall et al., 2010). This is a criterion met only by the dissolving pulp sample in the present work. The kraft pulp and the TEMPO-oxidized dissolving pulps are, to some degree, in conflict with the assumptions inherent in the model. For this reason, the NMR estimates of the specific surface area for the kraft and the TEMPO-oxidized samples should

Table 2
Water absorption capacity of composite materials.

Composite	(m(water))/(m(solid material))	(m(water))/(m(fibre))
Fibre/PMMA	0.13	0.66
Fibre/PBA	0.17	0.84
Fibre/PMMA (WD)	2.23	3.84
Fibre/PBA (WD)	2.44	6.10

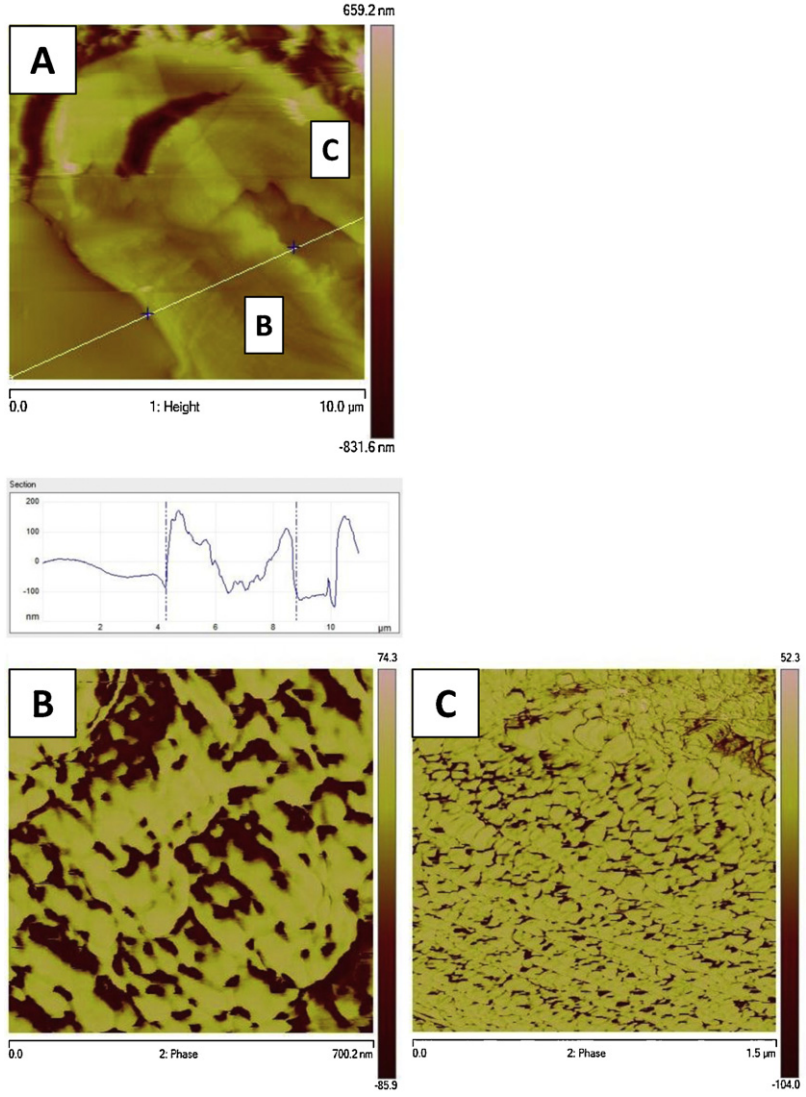

Fig. 6. AFM images of a cross-section of an in situ polymerized fibre-reinforced composite, i.e., fibre/PMMA. Image A is a height image showing the fibre wall with the corresponding surface roughness below. Image B is a phase image from the lower left side of the fibre wall (scale bar, 700 nm). Image C is a phase image from the upper right side of the fibre wall (scale bar, 1.5 μm). Two distinct phases can be detected in the fibre wall, the brighter areas corresponding to regions of higher stiffness.

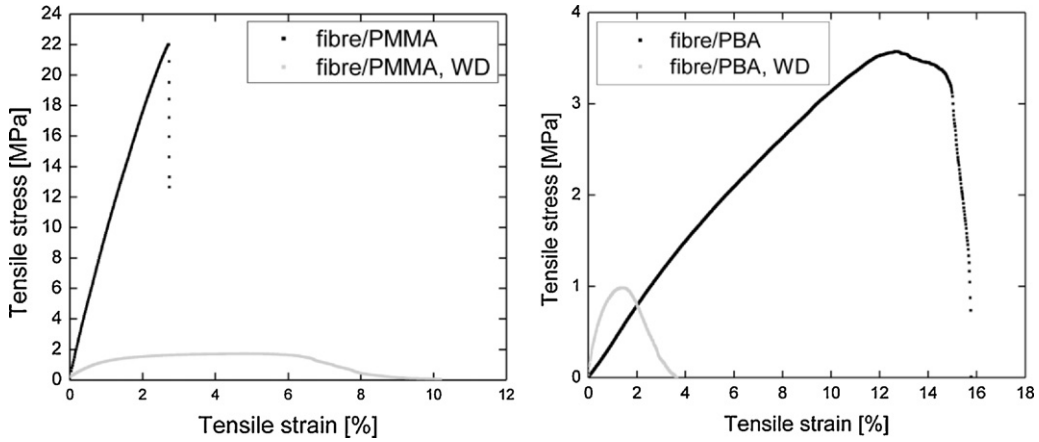

Fig. 7. Mechanical properties of the composite materials fibre/polymer (black) and the corresponding reference fibre/polymer WD (grey).

be considered only semi-quantitative estimates, probably underestimating the specific surface area in the water-swollen state. Taking this into consideration, and judging from the fact that air-dried dissolving pulp exposes a surface area as small as 1.6 $m^2 g^{-1}$, the combined NMR and BET results indicate that the liquid exchange procedure was quite successful in preserving a significant portion of the specific surface area available in the water-swollen state.

For the TEMPO-oxidized dissolving pulp, almost all the initially available surface area was preserved in the dry state, indicating that the developed method can be used to preserve, to a great extent, the water-swollen structure in the dry state.

Assuming a density of 1500 $cm^3 g^{-1}$ for cellulose, the specific surface area of 130 $m^2 g^{-1}$ corresponds to cellulose aggregates approximately 20 nm thick. It was concluded that the specific surface area in the dry state for this sample was high enough that it could be used as the scaffold for in situ polymerization in later work. It is clear from the structure shown in Fig. 3 that monomers can enter the pores in the fibre wall without having to diffuse through the solid cellulose fibrils.

This work tested two ways of drying samples to remove pentane, i.e., freeze drying and drying with inert gas. Due to the low freezing point of pentane, it could not be ascertained that pentane was removed by sublimation only, and since drying with gas was a convenient way of drying the samples, this method was chosen for the continuing work.

4.2. Distribution of polymers between fibres and throughout the fibre wall

The composites made of dry ultra-porous fibres are fairly transparent, indicating that fibril aggregates and polymers were thoroughly mixed on a nanoscale, since light scattering can almost be avoided. This also shows that a new type of fibre/polymer composite has indeed been formed where the fibrillar structure of the fibres (see Fig. 2B and C) has been interpenetrated by the different polymers. In turn this means that this composite is no longer a fibre-reinforced composite but a fibril-reinforced composite where the reinforcing elements are the cellulose nanofibrills inside the fibre wall and this has been achieved without the need to liberate the fibrils from the fibre wall. To the knowledge of the authors this has not been demonstrated before and constitutes a basis for further utilization of the delignified wood fibre wall as a scaffold for high value added products. This also means that wood fibres will have totally new application areas for material researchers.

The fibre content in the fibre/polymer sample is lower than in the fibre/polymer WD sample. This is most probably due to a filling of the open fibre wall network with polymer, resulting in a lower weight fibre fraction. It is worth mentioning that the samples contain approximately the same amount of fibres, since the starting material, in all cases, was sheets of the same grammage, i.e., 110 $g m^{-2}$.

The choice of monomers for the matrix polymers was made in order to work with an easily polymerized system and to distinguish between use of polymers with different glass transition temperatures (T_g). From the literature it is known that PMMA has a $T_g > 25\,^{\circ}C$ and PBA a $T_g < 25\,^{\circ}C$ (Marck, 2007). The absolute properties of the composites should therefore not be compared with the best available composites today. Instead the focus should be on relative comparison of the properties of the fibre-reinforced composites and the fibril-reinforced composites.

It was a delicate task to establish a method to determine the distribution of matrix polymer inside the fibre wall. It is naturally necessary to use methods with a nanoscale resolution, but it was also needed to prepare samples which can be analysed using the desired method. After evaluating various methods, it was found most suitable to cut the composites in thin microtome slices and to analyse these cross-sections using various microscopy techniques. AFM phase imaging can collect nanoscale-resolved information about regions in the material with different elasticity.

It was possible to cut the fibre/PMMA samples using a rotary microtome both with and without epoxy embedding; the cross-section of fibre/PMMA was thereafter analysed using SEM (see Fig. 5A) and AFM (see Fig. 6).

It was impossible to cut the fibre/PBA samples using a rotary microtome since the polymerization with PBA resulted in such a soft matrix surrounding the fibres. Even though the sample was embedded in epoxy, it was impossible to cut a thin film without smearing the matrix polymer. Since the epoxy could not penetrate into the composite, this was an early indication that the polymerization in the porous fibre structure was successful, i.e., most pores in the fibre wall structure had been filled with polymer, rendering a compact structure making it difficult for the epoxy to penetrate into the sample.

Fig. 5A shows that the fibres in the fibre/PMMA sample are dispersed in the PMMA matrix, and also that the lumen of the fibres are filled with polymer. The fibres are not completely evenly distributed in the matrix. The stripes in the image were probably caused by the knife from the microtome when preparing the cross-section. Fig. 5B and C shows that the cellulose aggregates are separated from each other and that they are covered by the matrix polymer.

When performing the AFM imaging of the cross-section of fibre/PMMA, it was possible to first locate the fibres in the matrix with an overview camera, so fibres in regions undisturbed by microtome knife marks could be selected for imaging. The height image (Fig. 6A) and the corresponding surface roughness profile in Fig. 6 show a fibre in PMMA matrix. The roughness profile indicates that the surface is smooth outside the fibre, corresponding to a cut through a pure PMMA section. Entering the fibre wall structure, the roughness increases, but reverts to a flat surface when entering the lumen, suggesting that the structure outside the fibre wall is similar to the structure in the lumen. This structure was indicated by the SEM image as well (see Fig. 5A).

The left part of the fibre wall is thicker than the right part of the fibre wall. Fig. 6B and C shows AFM phase images of the left and right parts of the fibre wall, where two phases are clearly present. In AFM phase images, brighter areas correspond to regions with higher stiffness in the material. The brighter parts most probably correspond to cellulose fibril aggregates and the darker parts to PMMA, distributed between the brighter cellulose aggregates. In Fig. 6C, the brighter parts are ordered in a typically lamellar structure. Although the magnification is not the same in Fig. 6B and C, it appears that the concentration of PMMA is higher in Fig. 6B than in C. The left side of the fibre contains more polymer, indicating that the impregnation of monomer is not homogeneous throughout the fibre structure. This would also explain the difference in fibre wall thickness observed in Fig. 6A. The rougher part of the surface profile corresponds to a fibre wall thickness of 5 μm.

The fibre/polymer samples display a drastic reduction in water absorption capacity compared with the fibre/polymer WD. The absorption capacity was first calculated as the amount of water per solid material, but since the samples differ in fibre content, the absorption capacity was also normalized with respect to fibre content. It is known from the literature that the monomer systems used in the present work shrink during polymerization; the fibre/polymer samples will not form a completely compact system as the shrinkage may induce some porosity, possibly located at the polymer–fibre phase boundaries. Regardless of how the absorption capacity is calculated, the composites containing PMMA as a matrix polymer, i.e., fibre/PMMA and fibre/PMMA WD, have a lower absorption capacity. This might be because PMMA is a much stiffer

polymer than is PBA, so the fibres are hindered by PMMA from swelling when soaked in water. The water-dried fibres can absorb water into the interior of the polymer-free fibre wall, so their water absorption capacity is significantly higher.

The mechanical properties were investigated to establish whether there was any difference in behaviour when polymerization was allowed to occur inside the fibre wall compared with the reference samples in which the fibre wall had been closed by drying from water. For both fibre/PMMA and fibre/PBA, tensile stress increased significantly even though the fibre content was lower for the samples than the reference samples, i.e., fibre/polymer WD. Attempts were made to press the fibre/polymer samples to increase the fibre content, but the pressing unfortunately led to a collapse of the open fibre structure. It was therefore not possible to compare samples of fibre/polymer with fibre/polymer WD at the same fibre content. Fibre/PBA is a more interesting composite material to analyse, since its fibre structure can reinforce the soft matrix more than in fibre/PMMA. Fibre/PBA displays a ductile behaviour that might be explained by a system in which the polymer and fibril aggregates are allowed to slide against each other. Some pores are available in the structure, as discussed in the previous section, which might help the two constituents to slide more easily when the sample is loaded. The results shows the importance of nano sized reinforcing element, in the case of fibrils in the fibre wall, compared to micro sized reinforcement, in the case of collapsed fibres in the reference samples. The results clearly indicate that the in situ polymerization inside the fibre wall resulted in a new type of fibre-reinforced composite and this demonstrates the great potential of using the inherent mechanical properties of the fibrils without having to consume considerable energy by mechanically disintegrating the fibre wall.

5. Conclusions

Dry ultra-porous fibre networks were obtained by subjecting wet fibre sheets to a liquid exchange procedure. This procedure was evaluated by comparing the specific surface area of the water-swollen starting material measured using NMR with the specific surface area of the dry ultra-porous fibres measured using BET.

The dry open structure was successfully used as a scaffold for in situ polymerization, allowing the mixing of fibrils in the fibre wall with matrix polymer at the nanoscale without disintegrating the fibre wall. These results demonstrate a new way of preparing fibril-reinforced composites in which the fibres can be oriented in the initial sheet before the liquid exchange and polymerization step. This will also allow for the use of the excellent properties of the cellulose nanofibrills, both regarding mechanical properties and specific surface area, without the need for mechanical disintegration of the fibre wall before use.

Acknowledgements

SCA Östrand AB and Domsjö Fabriker AB are acknowledged for their kind supply of the pulp used in this work. The authors would like to acknowledge Ann-Catrine Hagberg at Innventia for help with epoxy imbedding and preparing cross-sections with microtome, the electron microscopy unit at Karolinska Institutet for the FE-SEM analysis and Torbjörn Pettersson at Fibre and Polymer Technology, KTH, for help with AFM images. Wallenberg Wood Science Center is acknowledged for financial support.

References

Andreasson, B., Forsström, J., & Wågberg, L. (2005). Determination of fibre pore structure: Influence of salt, pH and conventional wet strength resins. *Cellulose*, *12*(3), 253–265.

Belgacem, M. N., & Gandini, A. (2008). *Monomers, polymers and composites from renewable resources*. Oxford: Elsevier Science.

Brunauer, S. E., Emmett, P. H., & Teller, E. (1938). Adsorption of gases in multimolecular layers. *Journal of the American Chemical Society*, *60*, 309–319.

Capadona, J. R., Van Den Berg, O., Capadona, L. A., Schroeter, M., Rowan, S. J., Tyler, D. J., et al. (2007). A versatile approach for the processing of polymer nanocomposites with self-assembled nanofibre templates. *Nature Nanotechnology*, *2*(12), 765–769.

Chunilall, V., Bush, T., Larsson, P. T., Iversen, T., & Kindness, A. (2010). A CP/MAS C-13-NMR study of cellulose fibril aggregation in eucalyptus dissolving pulps during drying and the correlation between aggregate dimensions and chemical reactivity. *Holzforschung*, *64*(6), 693–698.

Duchesne, I., & Daniel, G. (1999). The ultrastructure of wood fibre surfaces as shown by a variety of microscopical methods - a review. *Nordic Pulp & Paper Research Journal*, *14*(2), 129–139.

Eichhorn, S. J., Dufresne, A., Aranguren, M., Marcovich, N. E., Capadona, J. R., Rowan, S. J., et al. (2010). Review: Current international research into cellulose nanofibres and nanocomposites. *Journal of Materials Science*, *45*(1), 1–33.

Herrington, T. M., & Midmore, B. R. (1984). Adsorption of ions at the cellulose aqueous-electrolyte interface.2. Determination of the surface-area of cellulose fibers. *Journal of the Chemical Society – Faraday Transactions I*, *80*, 1539–1552.

Hsu, L., Weder, C., & Rowan, S. J. (2011). Stimuli-responsive, mechanically-adaptive polymer nanocomposites. *Journal of Materials Chemistry*, *21*(9), 2812–2822.

Hult, E. L., Larsson, P. T., & Iversen, T. (2001). Cellulose fibril aggregation – An inherent property of kraft pulps. *Polymer*, *42*(8), 3309–3314.

Katz, S., Beatson, R. P., & Scallan, A. M. (1984). The determination of strong and weak acidic groups in sulfite pulps. *Svensk Papperstidning*, *87*, R48–R53.

Klemm, D., Kramer, F., Moritz, S., Lindstrom, T., Ankerfors, M., Gray, D., et al. (2011). Nanocelluloses: A new family of nature-based materials. *Angewandte Chemie – International Edition*, *50*(24), 5438–5466.

Kohnke, T., Lund, K., Brelid, H., & Westman, G. (2010). Kraft pulp hornification: A closer look at the preventive effect gained by glucuronoxylan adsorption. *Carbohydrate Polymers*, *81*(2), 226–233.

Larsson, P. T., Wickholm, K., & Iversen, T. (1997). A CP/MAS C-13 NMR investigation of molecular ordering in celluloses. *Carbohydrate Research*, *302*(1-2), 19–25.

Lindström, T., & Carlsson, G. (1982). The effect of carboxyl groups and their ionic form during drying on the hornification of cellulose fibers. *Svensk Papperstidning-Nordisk Cellulosa*, *85*(15), R146–R151.

Marck, J. E. (2007). *Physical properties of polymers handbook*. New York: Springer.

Mendez, J., Annamalai, P. K., Eichhorn, S. J., Rusli, R., Rowan, S. J., Foster, E. J., et al. (2011). Bioinspired mechanically adaptive polymer nanocomposites with water-activated shape-memory effect. *Macromolecules*, *44*(17), 6827–6835.

Newman, R. H. (1992). Solid-state C-13 NMR-spectroscopy of multiphase biomaterials. *ACS Symposium Series*, *489*, 311–319.

Olsson, R. T., Samir, M., Salazar-Alvarez, G., Belova, L., Strom, V., Berglund, L. A., et al. (2010). Making flexible magnetic aerogels and stiff magnetic nanopaper using cellulose nanofibrils as templates. *Nature Nanotechnology*, *5*(8), 584–588.

Saito, T., Hirota, M., Tamura, N., Kimura, S., Fukuzumi, H., Heux, L., et al. (2009). Individualization of nano-sized plant cellulose fibrils by direct surface carboxylation using TEMPO catalyst under neutral conditions. *Biomacromolecules*, *10*(7), 1992–1996.

Stone, J. E., & Scallan, A. M. (1965). A study of cell wall structure by nitrogen absorption. *Pulp and Paper Magazine of Canada*, *66*, 407–414.

Stone, J. E., & Scallan, A. M. (1966). Influence of drying on the pore structures of the cell wall. In F. Bolam (Ed.), *Consolidation of the Paper Web: Transactions of the symposium held at Cambridge* September 1965, Vol. 1, (pp. 145–174).

Wågberg, L., & Björklund, M. (1993). Adsorption of cationic potato starch on cellulosic fibres. *Nordic Pulp & Paper Research Journal*, *8*(4), 339–404.

Wang, X. S., Maloney, T. C., & Paulapuro, H. (2003). Internal fibrillation in never-dried and once-dried chemical pulps. *Appita Journal*, *56*(6), 455–459.

Wickholm, K., Larsson, P. T., & Iversen, T. (1998). Assignment of non-crystalline forms in cellulose I by CP/MAS C-13 NMR spectroscopy. *Carbohydrate Research*, *312*(3), 123–129.